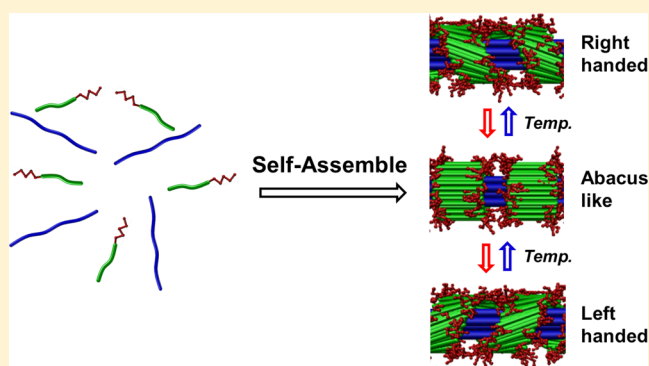


Superhelices with Designed Helical Structures and Temperature-Stimulated Chirality Transitions

Chunhua Cai,[†] Jiaping Lin,^{*,†} Xingyu Zhu,[†] Shuting Gong,[†] Xiao-Song Wang,^{*,‡} and Liquan Wang[†][†]Shanghai Key Laboratory of Advanced Polymeric Materials, State Key Laboratory of Bioreactor Engineering, Key Laboratory for Ultrafine Materials of Ministry of Education, School of Materials Science and Engineering, East China University of Science and Technology, Shanghai 200237, China[‡]Department of Chemistry, Waterloo Institute of Nanotechnology (WIN), University of Waterloo, Waterloo N2L 3G1, Canada

Supporting Information

ABSTRACT: The synthesis of multicomponent superhelices with determined chirality has been realized. By adding water to polymer solution in organic solvents (tetrahydrofuran/*N,N'*-dimethylformamide, THF/DMF), poly(γ -benzyl L-glutamate)-*block*-poly(ethylene glycol) (PBLG-*b*-PEG) are able to pack orderly around the surface of PBLG homopolymer bundles with designed helical structures, e.g., right-handed and left-handed, depending on THF/DMF ratio and temperature. A systematic investigation leads to the construction of a temperature–organic solvent composition phase diagram. Before the organic solvents were totally removed, the chirality of the assemblies can be reversibly switched using temperature stimulus. This temperature-stimulated chirality transition of polypeptide superhelices is unprecedented. Circular dichroism (CD) experiments indicated that the packing mode of pending phenyl groups from PBLG chain is responsible for the determination of the helical morphologies.



INTRODUCTION

Helical structure is ubiquitous in nature.^{1–3} For example, tobacco mosaic virus (TMV) has a type of core–shell superhelix that contains a RNA core and the coating proteins assemble into capsid with right-handed chirality.^{4,5} Although creating assemblies mimicking protein capsid structures has been intensively studied^{6–9} and polymeric supramolecular helices have been reported in several cases,^{10–20} TMV-like core–shell hierarchical superhelix is rarely reported.^{21–23} Particularly, chemistry for designed synthesis of TMV-like assemblies with tunable and temperature-stimulated chirality has not been explored.

Liu et al. discovered that poly(*n*-butyl methacrylate)-*block*-poly(2-cinnamoyloxyethyl methacrylate)-*block*-poly(*tert*-butyl acrylate) (PBMA-*b*-PCEMA-*b*-PtBA) triblock copolymer can self-assemble into both double and triple helices.¹¹ The superhelices have no preferred twisting sense. Both left-handed and right-handed helices were formed simultaneously. In another work, through coassembly of poly(acrylic acid)-*block*-poly(methyl acrylate)-*block*-polystyrene (PAA-*b*-PMA-*b*-PS) triblock copolymers with different multiamines, Pochan and co-workers have prepared a mixture of single and double superhelices with coexistence of left- and right-handedness.¹² Using chiral polymers, e.g. polypeptides as building blocks, superhelices with uniform handedness have been prepared.^{15–20} Nolte and co-workers discovered that both

polystyrene-*block*-poly(isocyanato-L-alanine-L-alanine) (PS-*b*-PIAA) and polystyrene-*block*-poly(isocyanato-L-alanine-L-histidine) (PS-*b*-PIAH) were able to self-assemble into helical superstructures.¹⁵ PIAA and PIAH segments have rigid α -helix conformation with right-handed and left-handed chirality, respectively, while the assembled superhelices have an opposite chirality to that of the constituent polypeptide segments in the copolymers. However, due to very limited examples, the formation mechanism of chiral polymers into superhelical structures is not clear, and the relationship between the chirality of the superhelix and the building chiral polymers has not been well explored yet.

Following recent progress in polymer multicomponent self-assembly,^{24–30} we have reported that poly(γ -benzyl L-glutamate)-*block*-poly(ethylene glycol) (PBLG-*b*-PEG) rod–coil block copolymers can cooperatively self-assemble with rigid PBLG homopolymers into TMV-like core–shell superhelical structures with the block copolymers wrapping around the polypeptide homopolymer bundles.^{31,32} Particularly, their chirality is highly uniform that all the superhelices are right-handed. By elevating the self-assembling temperature from 20 to 40 °C, the helical structures converted to a novel abacus-like

Received: October 13, 2015

Revised: December 8, 2015

Published: December 23, 2015

structure (beads-on-wire). Ordered packing of the rigid polypeptide segments is responsible for the assembling behavior as evidenced by computer simulations and previous literatures.^{31–36} The concept of assembling block copolymers with homopolymers into hierarchical structures has been followed by some research groups.^{37–40} For example, Manners, Winnik, and co-workers found that polyferrocenylsilane (PFS) homopolymers can effectively modify the self-assembly behavior of PFS-*b*-polyisoprene (PFS-*b*-PI) block copolymers in solution.³⁷ Pure block copolymers self-assembled into long cylindrical micelles, while the homopolymers form stacks of lamellar crystals. For the polymer mixtures, hierarchical structures with an elongated planar core and fiber-like protrusions were observed. In a very recent work, Novak et al. prepared superhelical structures from polycarbodiimide-*b*-PEG block copolymer and polycarbodiimide homopolymer mixtures.³⁸ Polycarbodiimide is a chiral rigid polymer with designed chirality. In their work, when the rod blocks and rod homopolymers in the mixtures possess the same chirality, superhelices with defined chirality (consistent with the chirality of the building blocks) were obtained. If the chirality of the rod blocks and rod homopolymers was mismatched, the helical feature cannot be distinguished. However, the formation mechanism of these superhelices has not been fully addressed.

In this work, as an effort to develop controlled self-assembly desirable for potential material applications,^{41,42} we continuously research into the system and realize the possibility for the synthesis of superhelices with determined and switchable chirality. Herein, we report our new findings that both right-handed and left-handed superhelices can be selectively synthesized depending on the preparation temperature and the common solvents (THF or DMF) used. A temperature–organic solvent composition phase diagram has been developed, which enriches our understanding on the system and is useful for designed synthesis of the hierarchical nanostructures. Before organic solvents are totally removed via dialysis, the chirality is temperature-sensitive and can be reversibly switched. The packing mode of phenyl groups pending on PBLG chains, which is sensitive to temperature and organic solvents, is an important parameter accounting for the observed phenomena.

■ EXPERIMENTAL SECTION

Reagents and Materials. α -Methoxy- ω -amino poly(ethylene glycol) (mPEG-NH₂, $M_n = 5000$) was purchased from Sigma-Aldrich. γ -Benzyl-L-glutamate-*N*-carboxyanhydride (BLG-NCA) was synthesized according to literatures.^{43,44} Triethylamine was refluxed with sodium and distilled immediately before use. All other chemicals were obtained from Adamas-beta and purified according to conventional methods or used as received.

Synthesis of PBLG Homopolymers and PBLG-*b*-PEG Block Copolymers. PBLG homopolymers and PBLG-*b*-PEG block copolymers were synthesized in anhydrous 1,4-dioxane solution using ring-opening polymerization of BLG-NCA initiated by anhydrous triethylamine and mPEG-NH₂ macroinitiator, respectively.^{43–45} The reaction was performed in flame-dried reaction bottle under a dry nitrogen atmosphere for 3 days at 15 °C. At the end of the polymerization, the reaction mixture was poured into a large volume of anhydrous ethanol. The precipitates were collected and dried under vacuum. The resulting products were purified twice by repeated precipitation from a chloroform solution into a large volume of anhydrous methanol. In the present work, PBLG₅₂₈₀₀₀ and PBLG₃₃₀₀₀₀-*b*-PEG₅₀₀₀ (subscripts denote M_n for each segment) were synthesized, and the polydispersity index (PDI) values are 1.15 and 1.21,

respectively. Details for the polymer synthesis and characterizations are presented in the [Supporting Information](#).

Aggregate Preparation. The aggregates were prepared by a selective precipitation method according to our previous work.^{31,32} First, block copolymers of PBLG-*b*-PEG and homopolymers of PBLG were respectively dissolved in tetrahydrofuran (THF), *N,N'*-dimethylformamide (DMF), or THF/DMF mixtures. The polymer concentration of the stock solutions is 0.25 g/L. Then 8 mL of block copolymer solutions and 2 mL of homopolymer solutions were mixed together. To the mixed solutions, 2.5 mL of deionized water was added at a rate of ca. 1 mL/min with vigorous stirring. Upon the addition of water, the colorless solution gradually became tint blue, which indicates the formation of aggregates. The solution was then dialyzed against deionized water for at least 3 days to remove organic solvents. All experimental procedures, including the processes of adding water and dialysis, were performed at a constant temperature. The polymer solutions, water for micellization, and water for dialysis were stored at a corresponding temperature for more than 12 h before use. The self-assembling experiments were conducted at various temperatures of 10–60 °C.

To study the temperature-induced reversible chirality transitions of superhelices, 8 mL of block copolymer solutions and 2 mL of homopolymer solutions were mixed together (initial solvent is THF/DMF = 1/1 in volume). To the mixed solutions, 1.5 mL of deionized water was added at a rate of ca. 1 mL/min with vigorous stirring. This process was performed at 20 °C. After stabilized for at least 10 h, the solution was annealed respectively at 40 and 60 °C for 10 h. Afterward, the solution was cooled back to 40 and 20 °C. At each temperature after annealing, samples for SEM and TEM were prepared and used to monitor the morphologies. In addition, to gain clear images, part of solution at each temperature was taken and dialyzed against water to freeze the morphologies.

Scanning Electron Microscopy (SEM). The surface profile of the aggregates was obtained from field emission SEM (S4800, Hitachi) operated at an accelerating voltage of 10 kV. The sample was prepared by placing drops of solution on a copper grid coated with carbon film and then were dried at room temperature. Before observation, the samples were sputtered by gold.

Transmission Electron Microscopy (TEM). The morphologies of aggregates were examined by field emission TEM (JEM-2100F, JEOL) operated at an accelerating voltage of 200 kV. Drops of solution were placed on a copper grid coated with carbon film and then were dried at room temperature. Before the observation, the sample was stained by phosphotungstic acid aqueous solution (0.5 wt %).

Cryo-TEM. Cryo-TEM samples were prepared in a controlled environment vitrification system (CEVS) at 25 °C. One drop of sample solution was placed on a copper grid coated with carbon film. The excess solution was blotted with a piece of filter paper, and then quickly dipped into liquid ethane, which was cooled by liquid nitrogen. The vitrified samples were then stored in liquid nitrogen until they were transferred to a cryogenic sample holder (Gatan 626) and examined with JEM-2200FS TEM (200 kV) at about –174 °C.

Atomic Force Microscopy (AFM). AFM images were obtained with XE-100 AFM instrument (Park Systems), employing the tapping mode. The samples were prepared by placing one drop of solution on a fresh-cleaved mica surface, and the sample was allowed to be dried in air.

Turbidity Measurements (OD). Turbidity measurements were performed to determine the critical water content (CWC) for the aggregation of polymers.^{46,47} PBLG-*b*-PEG block copolymers, PBLG homopolymers, and PBLG-*b*-PEG/PBLG polymer mixtures were dissolved in THF/DMF mixture solvent (1/1 in volume) with concentration of 0.25 g/L. 2 mL of each solution was introduced into a quartz cell (path length: 1 cm). Deionized water was then added drop by drop (ca. 0.01 mL per drop) with stirring. After each drop of deionized water was added, the solution was stirred for 1 min and then left to equilibrate for 2 min or more until the optical density was stable. The optical density (turbidity) was measured at a wavelength of 500 nm with a UV–vis spectrophotometer (UV-2550, Shimadzu).

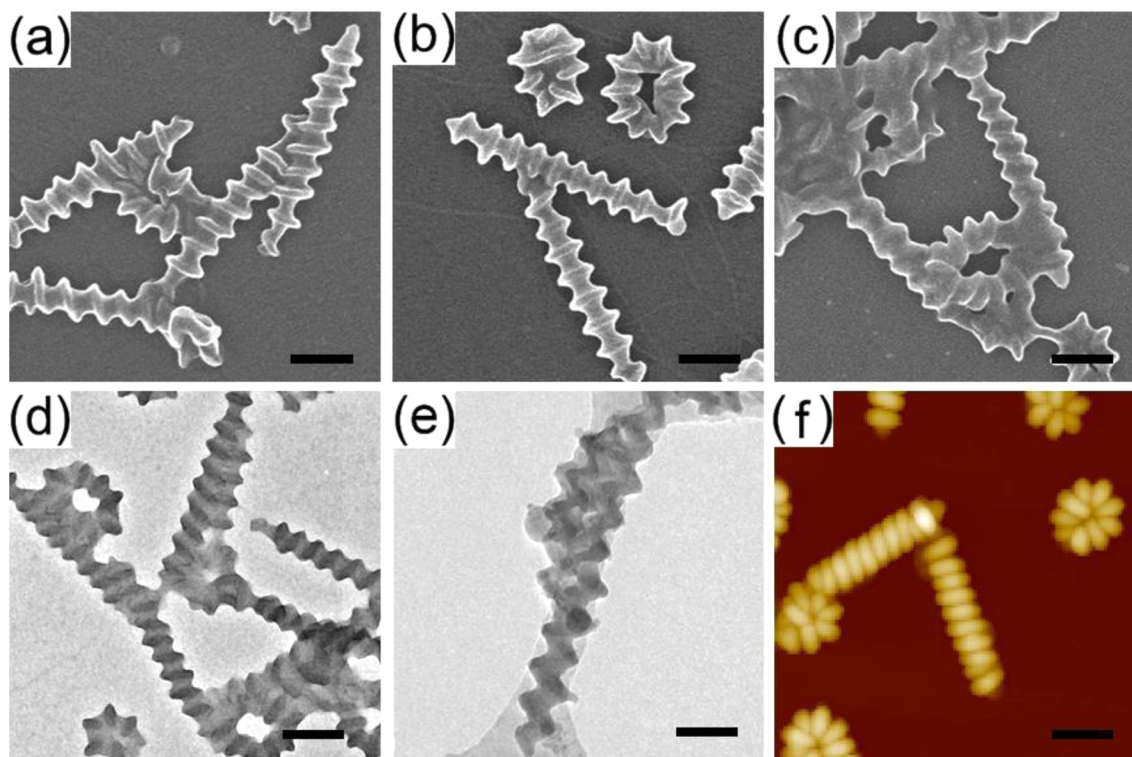


Figure 1. (a–c) SEM images of aggregates self-assembled from PBLG-*b*-PEG/PBLG mixtures at various preparation temperatures: (a) 20 °C, right-handed superhelices; (b) 40 °C, abacus-like structures; (c) 60 °C, left-handed superhelices. (d) TEM, (e) Cryo-TEM, and (f) AFM images for the left-handed superhelices prepared at 60 °C. The initial solvent is THF/DMF = 1/1 in volume. Scale bars: 250 nm.

Circular Dichroism (CD). CD analyses were performed with a JASCO J810 spectrometer at room temperature on aggregate solution in water. The diluted aggregate solutions (0.02 g/L for all the samples) were introduced in quartz cells with 1 cm optical path length. Wavelengths between 200 and 400 nm were analyzed, with an integration time of 1 s and a wavelength step of 0.2 nm.

RESULTS AND DISCUSSION

The aggregates were prepared by a selective precipitation method. First, PBLG-*b*-PEG and PBLG were dissolved in a mixed solvent of THF/DMF (1:1 by volume). Water was subsequently added at 20 or 40 °C, followed by dialysis to remove the organic solvents. At 20 °C, right-handed superhelices were obtained, while abacus-like structures were discovered at 40 °C (Figure 1a,b). These results are similar to our previous work.³¹ However, when we increased the preparation temperature to 60 °C, superhelices with left-handed chirality were exclusively observed. As shown in Figure 1c,d,f, all microscope images, including SEM, TEM, and AFM, reveal superhelices with left-handed chirality. Cryo-TEM further confirmed that this type of helices existed in solution (Figure 1e). As estimated from both SEM and TEM images, the diameter of the left-handed helices is about 140 nm with screw pitch of ca. 100 nm, which are similar to those for right-handed helices prepared at 20 °C. Out of this investigation, it is interesting to learn that the chirality for the superstructures can be varied depending on preparation temperature.

In order to develop knowledge on the system for possible designed synthesis, we performed further investigation on the effect of preparation conditions, e.g., assembling temperature and initial organic solvent composition, on the resulting morphologies. Since both polymers are soluble in either THF or DMF, we prepared a range of solutions with various volume

content of DMF in THF/DMF initial solvent (DMF vol %) from pure THF to 25, 50, 60, 70, 75, and 100 vol % of DMF. To these solutions, water was added drop by drop at different temperature from 10 to 60 °C. The organic solvents were subsequently removed by dialysis to freeze the assemblies. We then characterized morphologies for each sample using SEM. The resulting data are plotted into a morphology phase diagram, which reveals four characteristic zones: right-handed superhelices, abacus-like structures, left-handed superhelices, and plain fibers (Figure 2). As shown in the figure, when pure THF was used as initial solvent, right-handed superhelices are formed at all experimental temperature. By increasing the amount of DMF in the mixed solvents, experimental temperature required for the formation of right-handed structures dropped accordingly. After DMF content is over 70.0 vol %, no

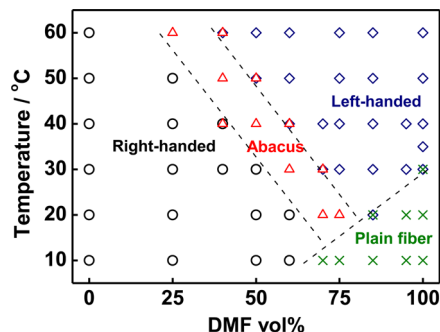


Figure 2. Morphology phase diagram of aggregates self-assembled from PBLG-*b*-PEG/PBLG mixtures as functions of temperature and initial solvent composition. The overlap of the two signs indicates the coexistence of two morphologies.

right-handed superhelices are observed, and left-handed structures start to form under most of conditions at higher temperature. At lower temperature, the resulting fibers have smooth surface, no helical structure were observed. PEG–water interactions are enhanced at lower temperatures.⁴⁸ This increased hydrophilicity of PEG renders the attraction between the PBLG segments relatively weaker.³¹ As a result, the PBLG segments from the block copolymers are packed randomly on the bundles of the PBLG homopolymers. The smooth surface is a consequence of this disordered packing of the PBLG segments. This rationalization is supported by our simulation work.^{31,32} The attraction forces between the rod/rod pair (ϵ_{RR}) are a parameter determining the morphology for the nanostructures self-assembled from the mixtures of rod–coil block copolymer/rod homopolymer. ϵ_{RR} is defined to be temperature related. At a smaller ϵ_{RR} , corresponding to a lower temperature, the simulations reveal plain fibers, and the rod–coil block copolymers randomly unwrap the bundles of the homopolymers.^{31,32} It is interesting to see that the right-handed zone at lower DMF vol % and the left-handed zone at higher DMF vol % are separated by a narrow band of abacus zone, and the boundaries move to higher temperature when DMF vol % decreases. This confirms that abacus-like structure is an intermediate morphology, and the formation of left-handed structures is favored in DMF-rich solvents at higher temperature. In addition, we have also studied the effect of PBLG length in PBLG-*b*-PEG on the phase diagram. As shown in Figure S1, when the molecular weight of the PBLG block in the block copolymers is relative smaller, the phase diagram shows no left-handed superhelix zone, and the boundary between right-handed superhelix and abacus zone shifts to higher DMF volume fractions. When the molecular weight of the PBLG block is relative larger, all morphologic zones are observed. Compared to the system with lower length of the PBLG block (Figure 1), the both boundaries for abacus/left-handed superhelix and abacus/right-handed superhelix move to lower DMF volume fractions.

To understand the effect of solvent in depth, we investigated helical angle θ of the assemblies as a function of solvent composition (Figure 3). θ is defined as the angle between the

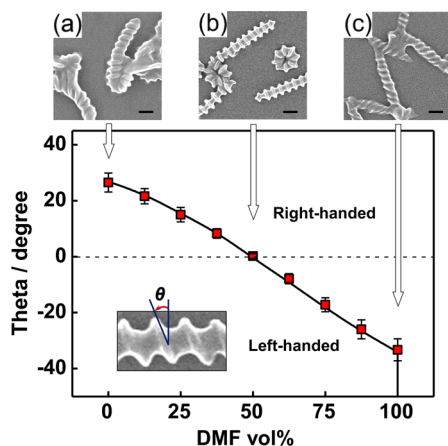


Figure 3. Dependence of the helical angle θ on the initial solvent composition. Inset is the definition of helical angle θ . SEM images represent the aggregates self-assembled from PBLG-*b*-PEG/PBLG mixtures with various content of DMF in THF/DMF initial solvent: (a) THF, (b) THF/DMF = 1/1, and (c) DMF. $T = 40$ °C. Scale bars: 250 nm.

screw and an axial line on its right as illustrated in the inset of Figure 3. The absolute θ value is associated with the chirality of the superhelices; i.e., higher absolute θ value means higher degree of chirality. The average θ value was obtained by measuring more than 100 assemblies for each sample. All samples were prepared using THF/DMF with various DMF content as initial solvents. The results are illustrated in Figure 3. As shown in Figure 3a, the angle for the right-handed helices is about +27.1° when pure THF was used as initial solvent. With increasing the amount of DMF in the mixed solvents, the helical angle continuously decreases and becomes zero when DMF content reaches 50.0 vol %, resulting in abacus-like structures (Figure 3b). Further increasing the volume of DMF, left-handed morphologies with increased helical angles are created. For the left-handed superhelices prepared with pure DMF as initial solvent (Figure 3c), the helical angle θ reaches ca. -32.2°.

As we reported before, all superhelical structures are frozen upon dialysis. However, before the dialysis, the morphology is sensitive to temperature. We prepared assemblies by adding water (15.0 vol % to initial solvent) to polymer solution (initial solvent: THF/DMF = 1/1 in volume) at 20 °C. Before dialyzing against water to freeze the nanostructures, we anneal the solution respectively at 40 and 60 °C to investigate the effect of temperature on the assembling (the annealing time is no less than 10 h). It was found that abacus-like structures and left-handed superhelices are obtained for the samples annealed at 40 and 60 °C, respectively. Particularly, it is interesting that the morphologies are reversibly switchable as stimulated by temperature. SEM images for this process are illustrated in Figure 4. As shown in the images, right-handed superhelices (Figure 4a) are converted to abacus-like structures by annealing the solution at 40 °C (Figure 4b); further annealing at 60 °C, left-handed superhelices are created (Figure 4c). When the samples, after annealed at 60 °C, were cooled back to lower temperature at 40 or 20 °C, all left-handed structures created at

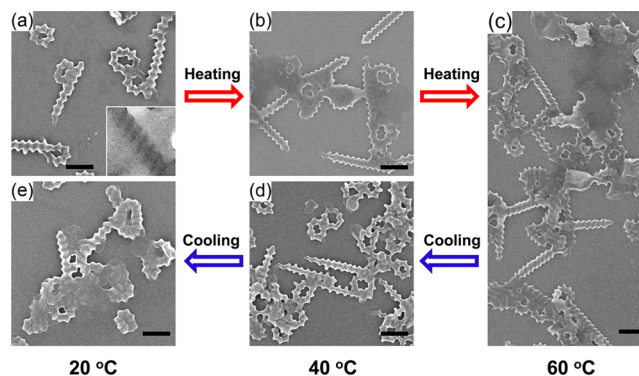


Figure 4. Temperature-induced reversible morphology transitions among right-handed, abacus-like, and left-handed superhelices. (a) Right-handed superhelices observed at 20 °C; (b) abacus-like structures obtained by heating the 20 °C solution to 40 °C; (c) left-handed superhelices obtained by heating the 40 °C solution to 60 °C; (d) abacus-like structures obtained by cooling the 60 °C solution to 40 °C; (e) right-handed superhelices obtained by cooling the 40 °C solution to 20 °C. The inset in (a) is a TEM image of the aggregate which is an enlarged image from Figure S2a. With each temperature variation, the solution was aged for at least 10 h. The initial solvent is THF/DMF = 1/1 in volume, and the added water content to organic solvent is 15.0 vol %. To gain clear images, we froze the equilibrated samples through dialysis at each observation point. Scale bars: 500 nm.

60 °C are converted back to abacus-like and right-handed morphologies, respectively (Figure 4d,e). Note that for the SEM experiments solvent was removed via dialysis after annealing at certain temperature. In order to rule out the possibility that the morphologies were altered during the process of dialysis, we also examined the samples right after annealing using TEM. A similar reversible morphology transformation as a function of annealing temperature was observed (see Figure S2 in Supporting Information).

Further analysis of the helical angle θ as a function of annealing temperature was performed. For the system with initial solvent of THF/DMF = 1/1 (in volume), the resulting data are plotted in Figure 5. As shown in the Figure 5, one can

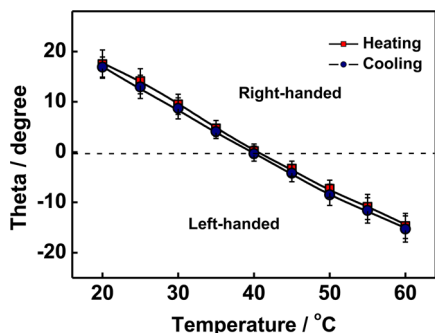


Figure 5. Dependence of the helical angle θ on temperature. At each observation temperature, the sample was equilibrated at least for 10 h. The initial solvent is THF/DMF = 1/1 in volume, and the added water content to organic solvent is 15.0 vol %. To gain clear images to analyze the helical angle θ , we froze the equilibrated samples through dialysis at each observation point.

see that the temperature is a parameter for helical angle turning from +18.2° at 20 °C to −15.3° at 60 °C. The change of the angle vector occurred around 40 °C. This is similar to the effect of solvent composition, and the θ value was reversible with the annealing temperature. In addition, we also observed morphology changes for the aggregates prepared in the system with THF/DMF = 1/3. As shown in Figure S3, abacus-like structures are assembled at 20 °C and left-handed superhelices are formed at 40 and 60 °C. Correspondingly, the helical angle gradually changes from 0° at 20 °C to −14.6° at 40 °C and then to −23.2° at 60 °C.

To better understand the effect of solvent and temperature on the self-assembly, the mechanism for the formation and transition of the superhelices was further investigated. We first measured critical water content (CWC), an indicative for the onset of aggregation, by recording abrupt changes in turbidity during water addition.^{46,47} As shown in Figure 6a, CWC for PBLG homopolymers, PBLG-*b*-PEG block copolymers, and PBLG-*b*-PEG/PBLG mixtures is 4.2, 7.5, and 5.0 vol %, respectively. Since CWC for PBLG homopolymers and PBLG-*b*-PEG/PBLG mixtures is very close, but much lower than that for PBLG-*b*-PEG block copolymers, it is reasonable to believe that in the process of adding water to the polymer mixture solution, PBLG homopolymers aggregated first followed by the surface absorption of PBLG-*b*-PEG block copolymers. Indeed, SEM image for the sample prepared from the solution at the point of CWC (5.0 vol % of water) shows fibers with smooth surfaces (Figure 6b). When water was further added and reached 10.0 vol %, surface of the fibers become rough (Figure 6c), suggesting PBLG-*b*-PEG block copolymers start to deposit

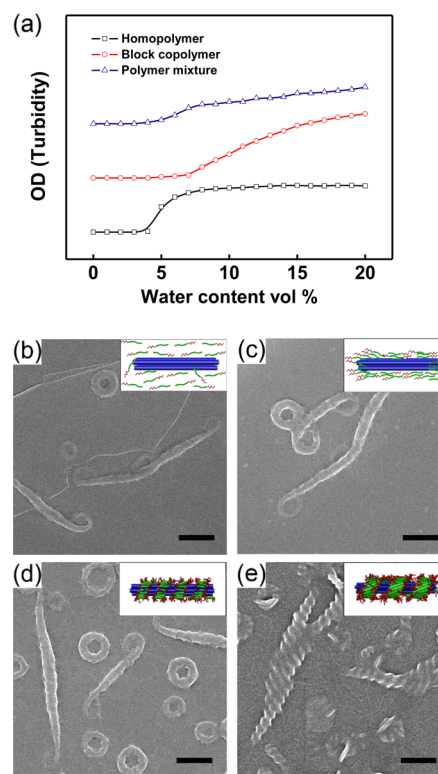


Figure 6. (a) Turbidity (optical density) curves of PBLG homopolymers, PBLG-*b*-PEG block copolymers, and PBLG-*b*-PEG/PBLG polymer mixtures as a function of the amount of water added to the solutions. (b–e) SEM images for self-assembled aggregates of PBLG-*b*-PEG/PBLG mixtures with various content of added water to organic solvent: (b) 5.0, (c) 10.0, (d) 20.0, and (e) 50.0 vol %. No dialysis was performed before SEM observation. The insets show the cartoon for the aggregates formed at corresponding added water contents. Scale bars: 300 nm.

onto the surface of PBLG homopolymer bundles. For the sample prepared from the solution containing 20.0 vol % of water, left-handed superhelices appear, suggesting that the block copolymers starts to pack into regular small-length structure on the surface of PBLG homopolymer bundles (Figure 6d). Further increasing water content to 50.0 vol %, left-handed superhelices can be clearly observed (Figure 6e).

It is well-known that PBLG with rigid chain are able to depending on environmental parameters, form either right-handed or left-handed cholesteric liquid crystals (LC) in high concentrated organic solutions. By increasing temperature or using better solvents for PBLG, the chirality of PBLG LCs usually undergoes a right- to left-handedness transition.^{49–51} It was observed that the transition of the LC chirality was associated with the chiral packing mode (handedness) of the phenyl groups pending on PBLG backbone. The transition of the chiral packing mode of the phenyl groups as a function of the nature of the solvent and temperature is mainly due to the variation of the dipole moment of solvents, which changes the dipole–dipole attraction (a kind of van der Waals force) between solvents and the phenyl groups pending from the PBLG homopolymers.^{49,52,53} Such cooperative chirality transition of phenyl group packing and LC is believed to minimize free energy.^{49,53,54} In our system, the PBLG homopolymer bundles with fiber-like structure are formed due to its low mobility in the presence of water (Figure 6b). Such bundles serve as templates for the self-assembly of PBLG-*b*-PEG block

copolymers. While during the process of PBLG segments in the block copolymers packing on the surface of the PBLG homopolymer bundles, the presence of water-soluble PEG chains may improve the mobility of PBLG segments facilitating their LC-like packing. Consequently, superhelical morphologies were observed. From the literature and our observations, we can therefore reasonably deduce that the chirality transition of the superhelices could be resulted from the change of chiral packing mode (handedness) of the pending phenyl groups as a function of organic solvents and temperature conditions used for the preparation of the aggregates.

The chiral arrangement of pending phenyl groups from PBLG segments can be detected using CD experiments. We therefore performed CD experiments for a number of superhelices prepared under various conditions, and their spectra are presented in Figure 7. It is clear that all samples

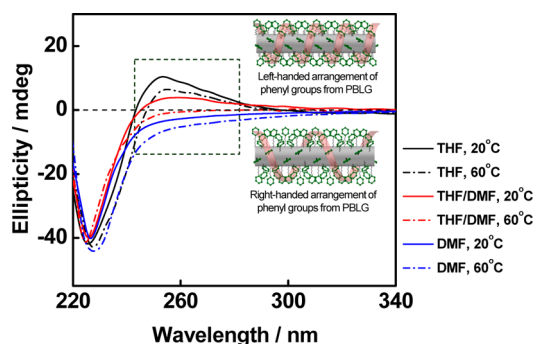
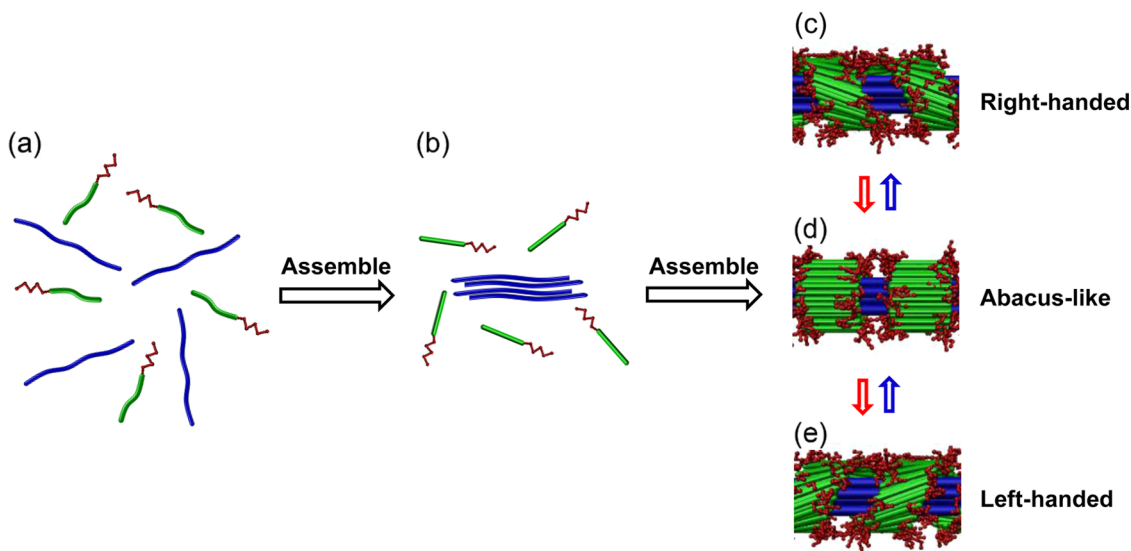


Figure 7. CD spectra of PBLG-*b*-PEG/PBLG assemblies as a function of organic solvents and temperature conditions. The insets show the schemes for the arrangement of phenyl groups in left-handed (upper) and right-handed (lower). The red helical belts indicate sense of the chiral arrangement of phenyl groups. The broken line square represents the CD spectra for the pending phenyl groups in different arrangements.

show a negative minimum around 220–230 nm due to PBLG chiral molecular backbone, suggesting that all aggregates are similar in the chirality of PBLG backbone.⁴⁹ When one pays attention to the signal at 240–280 nm region in the CD spectra, it is noticeable that the aggregates prepared from THF solution show positive signals, while those prepared from DMF show negative bands. According to previous studies, optical signal at this region represents the chirality originated from the arrangement of the pending phenyl groups. A positive band indicates left-handed arrangement, while a negative band corresponds to loosely packed right-handed form.^{49,52–54} Following this established knowledge, it can be deduced that phenyl groups in the block copolymers are packed in a left-handed fashion for the sample prepared from THF solution. This mode of phenyl group arrangement induces PBLG blocks pack in an opposite chirality, and right-handed superhelices are therefore observed (Figure 2). On the other hand, the observed left-handed superhelices for those prepared from DMF-rich solvents (Figure 2) are caused by right-handed arrangement of the phenyl groups. This is supported by the negative bands observed in Figure 7. For the samples obtained from THF/DMF mixture (1/1 in volume), the ellipticity is around zero (Figure 7), suggesting that the phenyl groups are arranged without strong preference of handedness, which corresponds to abacus-like morphology or superhelices with lower chirality intensity.

The chiral arrangement of the phenyl groups is also related to the preparation temperature. For the samples obtained from THF, at lower temperature (20 °C), the band intensity is higher than those prepared at higher temperature (60 °C) (Figure 7 and Supporting Information), suggesting that the chirality for the arrangement of the pending phenyl groups tends to be higher at lower temperature. In contrast, for the samples obtained from DMF, the absolute value of band intensity is higher at 60 °C than those at 20 °C, indicating the handedness for the phenyl group packing is increased with temperature. The observed trends in chirality as a function of temperature matches what observed in Figure 5. As shown in

Scheme 1. Formation Mechanism for the Superhelices with Different Chirality^a



^aThe blue, green, and red lines represent the PBLG homopolymers, PBLG segments, and PEG segments of block copolymers, respectively. See text and Figure 7 for a discussion on the assembling mechanism.

Figure 5, right-handed helices have high degree of chirality at lower temperature, while left-handed helices show high degree of chirality at higher temperature. When the aggregates are prepared from THF/DMF mixtures (1/1 in volume), the ellipticity of the bands approaches zero, as expected. Nevertheless, one can still evidently view that bands are changed from positive at 20 °C to negative at 60 °C, indicating the variation of chirality of phenyl group packing from left- to right-handed. This observation is in agreement with the chirality transition of superhelices as a function of temperature as illustrated in the phase diagram (Figure 2). For details of CD analysis, see Figure S4.

Based on the investigations, the assembly process is illustrated (Scheme 1). PBLG homopolymers and PBLG-*b*-PEG block copolymers are well dissolved in THF/DMF mixed solvents (Scheme 1a). When water was added to PBLG-*b*-PEG/PBLG mixtures in organic solvents, PBLG homopolymers quickly aggregate into fiber-like structures (Scheme 1b) and PBLG segments from block copolymers subsequently associated on the surface of homopolymer bundles, generating LC-like packing. As a result, superhelices are produced (Scheme 1c–e). The chirality of the superhelices is related to the handed arrangement of pendent phenyl groups from PBLG segments. In THF, the phenyl groups are left-handed arranged, which corresponds to the formation of right-handed superhelices. In DMF at relatively high temperature, the phenyl groups take loosely packed right-handed arrangement, resulting in left-handed superhelices. The regular packing of the pendent phenyl groups direct the arrangement of PBLG segments, which can reduce interfacial energy and optimize the penalty of the free energy change. As a result, by varying the organic solvents and adjusting temperature, polypeptide assemblies with designed morphologies can be synthesized and stimulated transformed.

CONCLUSION

In conclusion, our research has led to the possibility to synthesize multicomponent superhelices with determined chirality. By adding water to organic solutions, PBLG segments from PBLG-*b*-PEG block copolymers are able to wrap around PBLG homopolymer bundles and pack into ordered structures, generating chirality for the superstructures. It is found that the arrangement of phenyl groups pending on PBLG backbone is responsible for the chirality of the superhelices. Depending on common solvents used, e.g., THF, DMF, and THF/DMF, and preparation temperature, the handed arrangement of phenyl groups is observed to be associated with the chirality of formed superhelices. Consequently, right- or left-handed core-shell superhelices and their intermediated structure, abacus, can be prepared and stimulated-transformed in a designed fashion. This discovery enriches our capability in nanodesign of polypeptide assemblies.

ASSOCIATED CONTENT

Supporting Information

The Supporting Information is available free of charge on the ACS Publications website at DOI: 10.1021/acs.macromol.5b02254.

Polymer synthesis, TEM observation of temperature-induced reversible morphology transitions, and CD spectra of polypeptide aggregate solutions (PDF)

AUTHOR INFORMATION

Corresponding Authors

*(J.L.) E-mail: jlin@ecust.edu.cn.

*(X.-S.W.) E-mail: xiaosong.wang@uwaterloo.ca.

Notes

The authors declare no competing financial interest.

ACKNOWLEDGMENTS

This work was supported by the National Natural Science Foundation of China (51303055, 21234002, and 21474029), the National Basic Research Program of China (2012CB933600), and Research Fund for the Doctoral Program of Higher Education of China (20120074120001). Support from Projects of Shanghai municipality (15QA1401400, 15ZZ028, and 13JC1402000) is also appreciated. X.-S.W. thanks the NSERC and the University of Waterloo for financial support.

REFERENCES

- (1) Gal, J. *Chirality* **2011**, *23*, 1–16.
- (2) Liu, H.; Shen, X.; Wang, Z.-G.; Kuzyk, A.; Ding, B. *Nanoscale* **2014**, *6*, 9331–9338.
- (3) Yashima, E.; Maeda, K.; Lida, H.; Furusho, Y.; Nagai, K. *Chem. Rev.* **2009**, *109*, 6102–6211.
- (4) Bloomer, A. C.; Champness, J. N.; Bricogne, G.; Staden, R.; Klug, A. *Nature* **1978**, *276*, 362–368.
- (5) Klug, A. *Philos. Trans. R. Soc., B* **1999**, *354*, 531–535.
- (6) Xu, X.; Yuan, H.; Chang, J.; He, B.; Gu, Z. *Angew. Chem., Int. Ed.* **2012**, *51*, 3130–3133.
- (7) Xiong, X.; Uludag, H.; Lavasanifar, A. *Biomaterials* **2010**, *31*, 5886–5893.
- (8) Lee, E. S.; Kim, D.; Youn, Y. S.; Oh, K. T.; Bae, Y. H. *Angew. Chem., Int. Ed.* **2008**, *47*, 2418–2421.
- (9) Kwak, M.; Minten, I. J.; Anaya, D.-M.; Musser, A. J.; Brasch, M.; Nolte, R. J. M.; Mullen, K.; Cornelissen, J. J. L. M.; Herrmann, A. J. *Am. Chem. Soc.* **2010**, *132*, 7834–7835.
- (10) Sanchez-Ferrer, A.; Adamcik, J.; Mezzenga, R. *Soft Matter* **2012**, *8*, 149–155.
- (11) Dupont, J.; Liu, G.; Niihara, K.-i.; Kimoto, R.; Jinnai, H. *Angew. Chem., Int. Ed.* **2009**, *48*, 6144–6147.
- (12) Zhong, S.; Cui, H.; Chen, Z.; Wooley, K. L.; Pochan, D. J. *Soft Matter* **2008**, *4*, 90–93.
- (13) Cheng, L.; Lin, X.; Wang, F.; Liu, B.; Zhou, J.; Li, J.; Li, W. *Macromolecules* **2013**, *46*, 8644–8648.
- (14) Rowan, A. E.; Nolte, R. J. M. *Angew. Chem., Int. Ed.* **1998**, *37*, 63–68.
- (15) Cornelissen, J. J. L. M.; Fischer, M.; Sommerdijk, N. A. J. M.; Nolte, R. J. M. *Science* **1998**, *280*, 1427–1430.
- (16) Aggeli, A.; Nyrkova, I. A.; Bell, M.; Harding, R.; Carrick, L.; McLeish, T. C. B.; Semenov, A. N.; Boden, N. *Proc. Natl. Acad. Sci. U. S. A.* **2001**, *98*, 11857–11862.
- (17) Ho, R.-M.; Chiang, Y.-W.; Lin, S.-C.; Chen, C.-K. *Prog. Polym. Sci.* **2011**, *36*, 376–453.
- (18) Ho, R.-M.; Chiang, Y.-W.; Chen, C.-K.; Wang, H.-W.; Hasegawa, H.; Akasaka, S.; Thomas, E. L.; Burger, C.; Hsiao, B. S. J. *Am. Chem. Soc.* **2009**, *131*, 18533–18542.
- (19) Wang, Y.; Xu, J.; Wang, Y.; Chen, H. *Chem. Soc. Rev.* **2013**, *42*, 2930–2962.
- (20) Li, C. Y.; Cheng, S. Z. D.; Ge, J. J.; Bai, F.; Zhang, J. Z.; Mann, I. K.; Harris, F. W.; Chien, L.-C.; Yan, D.; He, T.; Lotz, B. *Phys. Rev. Lett.* **1999**, *83*, 4558–4561.
- (21) Percec, V.; Ahn, C.-H.; Ungar, G.; Yeardley, D. J. P.; Moller, M.; Sheiko, S. S. *Nature* **1998**, *391*, 161–164.
- (22) Brown, A. D.; Naves, L.; Wang, X.; Ghodssi, R.; Culver, J. N. *Biomacromolecules* **2013**, *14*, 3123–3129.
- (23) Rudick, J. G.; Percec, V. *Acc. Chem. Res.* **2008**, *41*, 1641–1652.

- (24) Zhu, J.; Zhang, S.; Zhang, K.; Wang, X.; Mays, J. W.; Wooley, K. L.; Pochan, D. J. *Nat. Commun.* **2013**, *4*, 2297.
- (25) Schacher, F.; Betthausen, E.; Walther, A.; Schmalz, H.; Pergushov, D. V.; Muller, A. H. E. *ACS Nano* **2009**, *3*, 2095–2102.
- (26) Bull, S. R.; Palmer, L. C.; Fry, N. J.; Greenfield, M. A.; Messmore, B. W.; Meade, T. J.; Stupp, S. I. *J. Am. Chem. Soc.* **2008**, *130*, 2742–2743.
- (27) Wang, X.; Guerin, G.; Wang, H.; Wang, Y.; Manners, I.; Winnik, M. A. *Science* **2007**, *317*, 644–647.
- (28) Moughton, A. O.; Hillmyer, M. A.; Lodge, T. P. *Macromolecules* **2012**, *45*, 2–19.
- (29) Petzetakis, N.; Dove, A. P.; O'Reilly, R. K. *Chem. Sci.* **2011**, *2*, 955–960.
- (30) Liu, Y.; Liu, B.; Nie, Z. *Nano Today* **2015**, *10*, 278–300.
- (31) Cai, C.; Li, Y.; Lin, J.; Wang, L.; Lin, S.; Wang, X.-S.; Jiang, T. *Angew. Chem., Int. Ed.* **2013**, *52*, 7732–7736.
- (32) Li, Y.; Jiang, T.; Lin, S.; Lin, J.; Cai, C.; Zhu, X. *Sci. Rep.* **2015**, *5*, 10137.
- (33) Cai, C.; Lin, J.; Zhuang, Z.; Zhu, W. *Adv. Polym. Sci.* **2013**, 259, 159–200.
- (34) Kros, A.; Jesse, W.; Metselaar, G. A.; Cornelissen, J. J. L. M. *Angew. Chem., Int. Ed.* **2005**, *44*, 4349–4352.
- (35) Lee, M.; Cho, B.-K.; Zin, W.-C. *Chem. Rev.* **2001**, *101*, 3869–3892.
- (36) Pinol, R.; Jia, L.; Gubellini, F.; Levy, D.; Albouy, P.-A.; Keller, P.; Cao, A.; Li, M.-H. *Macromolecules* **2007**, *40*, 5625–5627.
- (37) Cambridge, G.; Gonzalez-Alvarez, M. J.; Guerin, G.; Manners, I.; Winnik, M. A. *Macromolecules* **2015**, *48*, 707–716.
- (38) Reuther, J. F.; Siriwardane, A.; Campos, R.; Novak, B. M. *Macromolecules* **2015**, *48*, 6890–6899.
- (39) Cauchois, O.; Segura-Sanchez, F.; Ponchel, G. *Int. J. Pharm.* **2013**, *452*, 292–299.
- (40) Wu, S.; Wang, L.; Kroeger, A.; Wu, Y.; Zhang, Q.; Bubeck, C. *Soft Matter* **2011**, *7*, 11535–11545.
- (41) Qiu, H.; Russo, G.; Rupa, P. A.; Chabanne, L.; Winnik, M. A.; Manners, I. *Angew. Chem., Int. Ed.* **2012**, *51*, 11882–11885.
- (42) Groschel, A. H.; Schacher, F. H.; Schmalz, H.; Borisov, O. V.; Zhulina, E. B.; Walther, A.; Muller, A. H. E. *Nat. Commun.* **2012**, *3*, 710.
- (43) Lin, J.; Abe, A.; Furuya, H.; Okamoto, S. *Macromolecules* **1996**, *29*, 2584–2589.
- (44) Jeong, Y.-I.; Nah, J.-W.; Lee, H.-C.; Kim, S.-H.; Cho, C.-S. *Int. J. Pharm.* **1999**, *188*, 49–58.
- (45) Cai, C.; Wang, L.; Lin, J.; Zhang, X. *Langmuir* **2012**, *28*, 4515–4524.
- (46) Yu, Y.; Zhang, L.; Eisenberg, A. *Macromolecules* **1998**, *31*, 1144–1154.
- (47) Zhuang, Z.; Cai, C.; Jiang, T.; Lin, J.; Yang, C. *Polymer* **2014**, *55*, 602–610.
- (48) Bhargava, P.; Tu, Y.; Zheng, J. X.; Xiong, H.; Quirk, R. P.; Cheng, S. Z. D. *J. Am. Chem. Soc.* **2007**, *129*, 1113–1121.
- (49) Uematsu, I.; Uematsu, Y. *Adv. Polym. Sci.* **1984**, *59*, 37–74.
- (50) Watanabe, J.; Nagase, T. *Macromolecules* **1988**, *21*, 171–175.
- (51) Toriumi, H.; Kusumi, Y.; Uematsu, I.; Uematsu, Y. *Polym. J.* **1979**, *11*, 863–869.
- (52) Ishimuro, Y.; Hamada, F.; Nakajima, A. *Macromolecules* **1978**, *11*, 382–387.
- (53) Huang, C.-J.; Chang, F.-C. *Macromolecules* **2008**, *41*, 7041–7052.
- (54) Losik, M.; Kubowicz, S.; Smarsly, B.; Schlaad, H. *Eur. Phys. J. E: Soft Matter Biol. Phys.* **2004**, *15*, 407–411.